

# Structure and electronic properties of “DNA–gold–nanotube” systems: A quantum chemical analysis

P. Pannopard<sup>a,b,c</sup>, P. Khongpracha<sup>a,b,c</sup>, M. Probst<sup>d</sup>, J. Limtrakul<sup>a,b,c,\*</sup>

<sup>a</sup>Physical Chemistry Division, Department of Chemistry, Faculty of Science, Kasetsart University, Bangkok 10900, Thailand

<sup>b</sup>Center of Nanotechnology, Kasetsart University Research and Development Institute, Bangkok 10900, Thailand

<sup>c</sup>NANOTEC Center of Excellence, National Nanotechnology Center Kasetsart University, Bangkok 10900, Thailand

<sup>d</sup>Institute of Ion Physics and Applied Physics, Innsbruck University, Technikerstraße 25, 6020 Innsbruck, Austria

Received 23 July 2007; received in revised form 13 September 2007; accepted 13 September 2007

Available online 19 September 2007

## Abstract

The development of novel DNA sensors is a crucial issue in the diagnosis of pathogenic and genetic diseases. We have used density functional theory (DFT) to investigate the performance of hybrid DNA sensors consisting of a gold atom (Au) deposited on two types of single-walled carbon nanotubes: armchair SWCNT(8,0)/Au and zigzag SWCNT(5,5)/Au and compared these with bare Au. We also chose adenine:thymine (A:T) as a Watson–Crick base pair of the DNA double helix. In the recognition probe, SWCNT/Au/A, adenine is immobilized on the SWCNT/Au supporter via its active N7 anchor point. After thymine hybridization (SWCNT/Au/A:T), the overall modulations compared with the original systems. Due to the complimentary functions of gold, which acts as a powerful electron withdrawing and transmitting group and of the SWCNTs, which act as electron collecting centers, respectively, the hybrid systems, “SWCNTs/Au”, were found to exhibit more stability and sensitivity than the Au center alone. The changes in the HOMO–LUMO band gaps and in the atomic partial charges upon binding of thymine were rather small, but the change of the overall dipole moment was considerably larger in SWCNT/Au/A than it was in Au/A alone. The overall results suggest that the “SWCNTs/gold” system is a potential candidate for a nanostructure-based DNA sensor.

© 2007 Elsevier Inc. All rights reserved.

**Keywords:** DNA sensor; Density functional theory (DFT); Single-walled carbon nanotube (SWCNT); Gold atom; Adenine:thymine base pair (A:T)

## 1. Introduction

The idea of chemical sensing based on molecular recognition, even though still in an early developmental stage, is considered to be one of the most promising concepts for single-molecule detection. This approach requires probes which hold a specific recognition of desired chemical species and a transduction ability of that recognition incident into a quantitative response signal. Therefore, a chemical sensing probe that integrates both recognition and transduction moieties into a single molecular assembly would probably be a very versatile tool indeed. This scheme has been examined in various disciplines, especially for a nature imitating detection of

specific DNA sequences [1–4]. Gold nanoparticles (Au NPs) can have properties like high sensitivity and electrical conductivity as well as size-dependent optical capability and affinity to biomolecules [5–8]. Recent experimental and theoretical studies reported that amongst the nucleotides, adenine base has the highest affinity to gold particles [9] and preferentially binds to a nitrogen atom at the N7 position [10]. Furthermore, there is considerable interest in applying carbon nanotubes (CNTs) as charge-transport centers for electronic transducers [11–15]. Hence, several experiments have focused on the deposition of Au NPs onto CNTs [16–19] and there is increasing attraction to exploit a compatible assembly of them as nanoscale building-blocks for DNA detection [20]. Nevertheless, there is a lack of theoretical studies on the combinations of Au NPs, CNTs and DNA molecules.

It is the objective of the current work to investigate the modulation of adenine–thymine (A:T) hybridization interacting with a hybrid structure consisting of a gold atom as the reactive site for anchoring of the DNA bases on single-wall

\* Corresponding author at: Physical Chemistry Division, Department of Chemistry, Faculty of Science, Kasetsart University, Bangkok 10900, Thailand. Tel.: +66 294 28900x304; fax: +66 294 28900x324.

E-mail address: [fscjrl@ku.ac.th](mailto:fscjrl@ku.ac.th) (J. Limtrakul).

carbon nanotubes (SWCNTs, zigzag (8,0) and armchair (5,5)) as electron transfer supports. Additionally, electronic responses in the system are observed. This theoretical study shall provide support information for experimental results. We are aware that experimentally metal clusters normally serve as junctions. Nevertheless, single-atom junctions have been produced and measured experimentally and they are often investigated theoretically and computationally as important and well-defined prototypes.

## 2. Computational method

Table 1 compares several density functional/basis set combinations with respect to geometries and bonding energies of A:T. It can be seen that the results are not very sensitive to the particular choice. Since our system consists of about 150 atoms we choose the Perdew, Burke and Ernzerhof (PBE) [21] non-local generalized gradient functional (GGA), which is still computationally feasible. We found it necessary to use at least the cc-pVTZ basis set for reliable results. All subsequent calculations were performed using density functional theory with the PBE GGA functional. Dunning's correlation consistent polarized valence basis sets cc-pVDZ and cc-pVTZ were employed for SWCNTs and for the A:T base pair moiety, respectively. The electrons of Au were represented by a relativistic effective potential (ECP) [22] and (7s6p5d)/[6s3p2d] basis set was used for its 19 valence electrons. Except for some results in Table 1 where Gaussian 03 [23] was used, all calculations were performed with the Turbomole 5.7 code [24]. The Coulomb interactions were treated by the resolution of the identity (RI) technique [25]. We did not employ the basis-set superposition correction since the main emphasis of the work is the study of molecular responses in terms of charge rearrangements and of similar properties.

The configurations and their standard labeling are illustrated in Fig. 1. The semiconductor SWCNT(8,0) is comprised of 96 carbon atoms. Hydrogen terminates dangling orbitals at the tube ends. An electronically comparable model, metallic SWCNT(5,5) with 90 carbon atoms, is also chosen to make a comparative study. The most stable structure of gold species attached to each type of SWCNT was examined before taking it to construct the DNA probe. Our model systems are divided into four subsystems: a SWCNT, a gold atom (Au) and the two

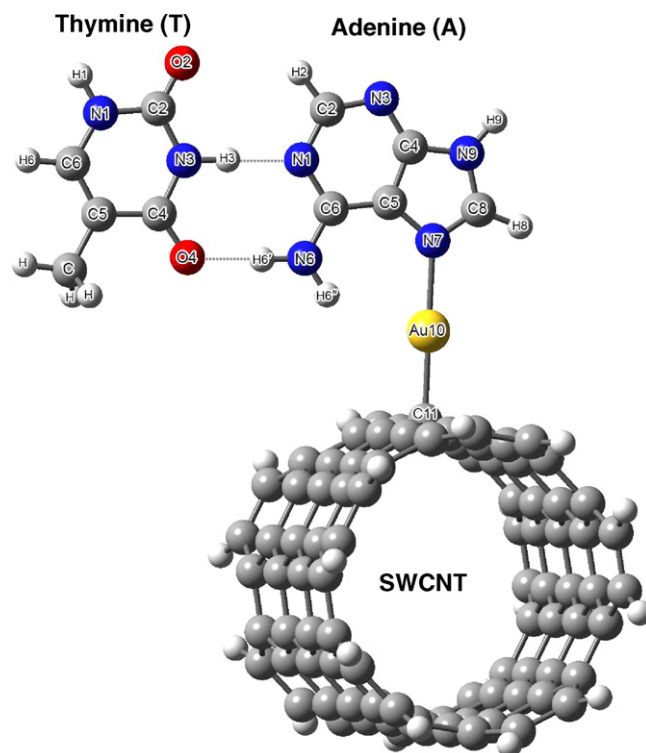


Fig. 1. Illustration of the SWCNT/Au/A:T system with standard numbering of the A:T base pair.

bases (A,T). The total binding energy ( $E_{tb}$ ) and the several two-body binding energies ( $E_b$ ) are defined according to the following equations:

$$E_{tb}(\text{SWCNT} \cdots \text{Au} \cdots \text{A} \cdots \text{T}) = E(\text{SWCNT/Au/A:T}) - E(\text{SWCNT}) - E(\text{Au}) - E(\text{A}) - E(\text{T}) \quad (1)$$

$$E_b(\text{SWCNT/Au/A} \cdots \text{T}) = E(\text{SWCNT/Au/A:T}) - E(\text{SWCNT/Au/A}) - E(\text{T}) \quad (2)$$

$$E_b(\text{SWCNT/Au} \cdots \text{A:T}) = E(\text{SWCNT/Au/A:T}) - E(\text{SWCNT/Au}) - E(\text{A:T}) \quad (3)$$

Table 1  
Comparison of methods and basis sets for the adenine–thymine base pair geometry and energy

Method	Bond lengths (Å)		Angles (°)		$E_b$ (A:T) (kcal/mol)
	$r(\text{N1} \cdots \text{N3})$	$r(\text{N6} \cdots \text{O4})$	$\angle(\text{N1H1N3})$	$\angle(\text{N6H6'O4})$	
Experiment	2.82 <sup>a</sup>	2.95 <sup>a</sup>	–	–	12.1 <sup>b</sup>
B3LYP/6-31G**	2.85	2.94	179.8	174.5	17.5
B3LYP/cc-pVDZ	2.85	2.94	179.8	174.4	18.0
BP86/cc-pVDZ	2.78	2.85	179.9	175.4	18.5
PBE/cc-pVDZ	2.78	2.86	179.8	175.0	20.4
BP86/cc-pVTZ	2.83	2.86	179.0	176.1	14.7
PBE/cc-pVTZ	2.82	2.88	179.6	174.7	16.4

<sup>a</sup> X-ray crystallographic measurements by Seeman et al. [26].

<sup>b</sup>  $\Delta H_{\text{exp}}$  for adenine–thymine with 9-methyladenine and 1-methylthymine from the mass spectrometry results of Yanson et al. [27].

$$E_b(\text{SWCNT} \cdots \text{Au/A : T}) = E(\text{SWCNT/Au/A : T}) - E(\text{SWCNT}) - E(\text{Au/A : T}) \quad (4)$$

$E$  without subscript denotes the total energy of each subsystem or complex.

### 3. Results and discussion

#### 3.1. SWCNT/gold complex (hybrid nanostructure)

The combination of CNT and gold is an advanced material which can form suitable supports for DNA sensors. This section describes the characteristics of the Au atom deposited on SWCNT(8,0) and SWCNT(5,5). In a previous work, Durgun et al. [28] calculated the adsorption of a single Au atom on semiconductor (SWCNT(8,0)) and metallic (SWCNT(6,6)) SWCNTs. They reported that the most favorable binding sites for the Au atom was the A–T site on SWCNT(8,0) and the T site on SWCNT(6,6) (A above axial C–C bond and T above the carbon atom) with Au–C bond lengths of 2.2 and 2.3 Å, respectively. We investigated the behavior of a single Au atom on SWCNT(8,0) and SWCNT(5,5) similar to what Durgun et al. did for a differently sized SWCNT. The possible positions for Au deposition are depicted in Fig. 2.

Fig. 3 shows all possible assemblies together with their binding energies of SWCNT(8,0)/Au and SWCNT(5,5)/Au complexes which are symmetrically optimized. It can be seen that the most stable Au binding occurs on the top site for both SWCNTs. Both on-top complexes with  $C_s$  symmetry were reoptimized without constraints (Fig. 4a and b). The Au positions and the Au–C bond distances (2.18 Å in both complexes) from our calculation are quite similar to those of Durgun's et al. Both SWCNT(8,0) and SWCNT(5,5) show no charge transfer to and from Au. (cf. Table 2). The Au atom binds with each of the surfaces with binding energies of 23.1 and 21.5 kcal/mol for SWCNT(8,0)/Au and SWCNT(5,5)/Au complexes, respectively.

#### 3.2. SWCNT/gold/adenine complexes (DNA sensor probe)

The SWCNT/gold system might act as an appropriate transducer to improve DNA sensor efficiency for the adsorption

of single stranded nucleic acid and the amplification of the double stranded hybridization signal and it might be a sensing material for nucleic acids (our target is adenine). This section deals with the immobilization of the adenine base on the support. The optimized geometries are depicted in Fig. 5 and the parameters (intermolecular bond length, binding energy and atomic partial charges) are tabulated in Table 2 for all complexes. The partial charges were calculated from the Mulliken analysis and via the natural population analysis (NPA) method [29]. For technical reasons, the latter was used with the LANL2DZ basis set for Au [30]. We also take into account the Au/A and Au/A:T complexes as references (Fig. 5).

##### 3.2.1. DNA probe stability

From Table 2, it can be seen that the Au–N7 and Au–C11 bond lengths are sensitive to base pair formation. The Au–N7 bonds are contracted from 2.26 Å in Au/A to 2.14 Å in both the SWCNT(8,0)/Au/A and SWCNT(5,5)/Au/A complexes. Similar results are found for the Au–C11 bond where the formation of A:T causes the Au–C11 bond to shorten from 2.18 to around 2.12 Å in both SWCNT(8,0)/Au and SWCNT(5,5)/Au systems. This is relevant for the effectiveness of the Au/SWCNT for being a steady probe because it enhances the immobilization of the recognition layer via a cooperative effect that strengthens the binding between SWCNT's, gold particles and DNA adenine. In considering the energetic results, it should be noted that both types of SWCNTs improve the strength of the interaction between the gold atom and the adenine base. In comparison to the Au/A complex, the binding energies between the gold atom and the adenine base are increased by 5.1 kcal/mol in the SWCNT(8,0)/Au/A complex and by 8.3 kcal/mol in the SWCNT(5,5)/Au/A complexes. Likewise, the interaction between the gold atom and the SWCNT, increases after interacting with the adenine base by 5.1 and 8.4 kcal/mol in SWCNT(8,0)/Au/A and SWCNT(5,5)/Au/A complexes, respectively, when compared with the SWCNT/Au system. Again, the SWCNT(8,0)/Au/A and SWCNT(5,5)/Au/A complexes are very similar to each other. It seems that SWCNT/Au hybrid structures are effective nanomaterials for adenine immobilization and adenine itself can bind to thymine efficiently. The atomic partial charges are also shown in Table 2. Au and SWCNT withdraw electrons from the adenine molecule. The polarization can be explained qualitatively by the electron affinity of the gold atom (2.31 eV) and by the one

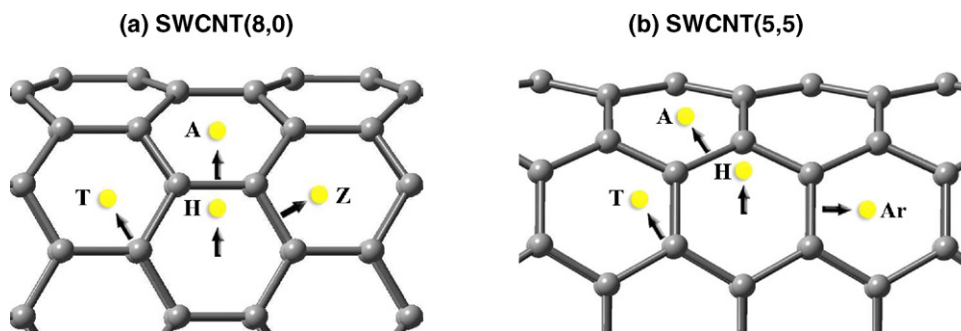
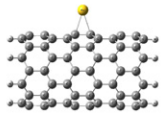
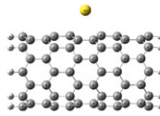
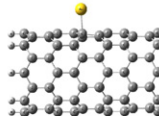
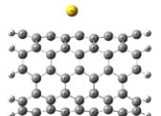
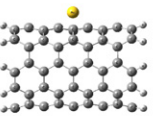
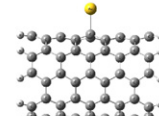


Fig. 2. Binding sites (H, hollow; A, axial; Z, zigzag; T, top; Ar, armchair) for adatoms adsorbed on SWCNT(8,0) and SWCNT(5,5).

SWCNT(8,0)/Au			
Axial	Zigzag	Hexagonal (Hollow)	Top
$C_{2v}$	$C_1$	$C_{2v}$	$C_s$
$E_b = 14.0$ kcal/mol	SCF not converging	$E_b = 13.5$ kcal/mol	$E_b = 23.5$ kcal/mol
			
SWCNT(5,5)/Au			
Axial	Armchair	Hexagonal (Hollow)	Top
$C_1$	$C_{2v}$	$C_{2v}$	$C_s$
$E_b = -0.8$ kcal/mol	$E_b = 13.2$ kcal/mol	SCF not converging	$E_b = 21.6$ kcal/mol
			

$$E_b = E_b(\text{SWCNT} \cdots \text{Au})$$

Fig. 3. Optimized geometries and calculated binding energies ( $E_b$ ) of SWCNT(8,0)/Au and SWCNT(5,5)/Au complexes.

of SWCNT (about 4 eV) as well as their charge-transport features after binding to adenine. Au is not only a good linker but also enhances electron transfer from the adenine base to the SWCNT, which leads to an electron loss on Au and adenine by 0.12e and 0.27e (calculated from Mulliken charge differences), respectively, and a corresponding negative charge on the SWCNT in both types of the SWCNTs/Au/A complexes.

### 3.2.2. Nucleic acid sensor sensitivity

In the previous subsection it was noted that electron density is transferred from adenine to the SWCNT. The SWCNT/Au system can withdraw about 0.1e more electron density from adenine than a bare Au. Here we report the modulation of the energy gap between the HOMO and LUMO of the systems. Opposite alterations of the energy gap in the Au probe (+0.13 eV) and in the SWCNT(8,0)/Au complexes when capturing the adenine base (−0.03 eV) are found. These events infer that the electron transfer rate in the SWCNT(8,0)/Au/A

system is enhanced and is also greater than in the Au/A complex due to the smaller energy gap in SWCNT(8,0)/Au/A (cf. Table 2). The SWCNT(5,5)/Au complex is insensitive to energy gap changing, but it can induce the electron transfer from the adenine base with better capability than the Au single atom. From the overall results, the Au single atom and SWCNT(8,0)/Au hybrid material provide different characteristics of the electronic signal. After binding with the adenine molecule, the electrical flow in the Au sensing system decreases (more resistance), while in the SWCNT(8,0)/Au one it increases (more conductance). Of course, the SWCNT(8,0)/Au system is more practical than the bare Au system in terms of signal transmission and its better thymine capturing and immobilization capability (see below).

### 3.2.3. Thymine hybridization

This topic is related to the information in Table 3 which elaborates the key parameters of the adenine base in all probe

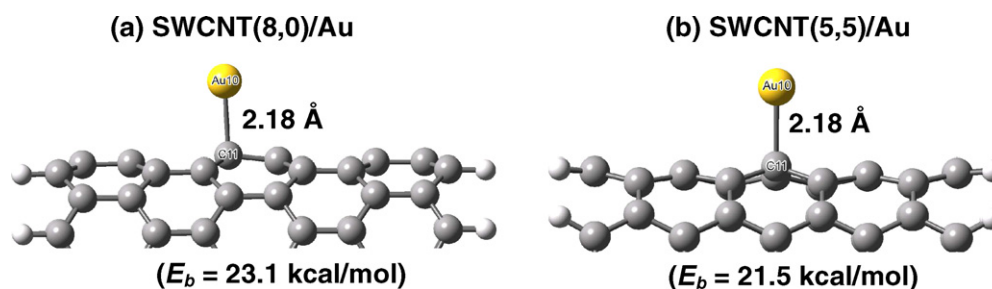


Fig. 4. Fully optimized geometries, calculated binding energies ( $E_b$ ) and Au-SWCNT distances of the most stable structure of (a) SWCNT(8,0)/Au and (b) SWCNT(5,5)/Au complexes.

Table 2  
Geometrical parameters (Å), calculated binding energies ( $E_b$ ; kcal/mol), energy gap (eV), molecular charges (au.) and dipole moment (debye) of Au/A:T, SWCNT(8,0)/Au/A:T, SWCNT(5,5)/Au/A:T and their fragments

	Au/A	Au/A:T	SWCNT/Au		SWCNT/Au/A		SWCNT/Au/A:T	
			SWCNT (8,0) complexes	SWCNT (5,5) complexes	SWCNT (8,0) complexes	SWCNT (5,5) complexes	SWCNT (8,0) complexes	SWCNT (5,5) complexes
Distance (Å) and energy (kcal/mol)								
$r(\text{N7-Au})$ , ( $E_b(\text{SWCNT/Au} \cdots \text{A:T})$ )	2.26 (14.1)	2.26 (13.4)	–	–	2.14 (19.2)	2.14 (22.4)	2.14 (18.3)	2.14 (22.0)
$r(\text{Au-C11})$ , ( $E_b(\text{SWCNT} \cdots \text{Au/A:T})$ )	–	–	2.18 (23.1)	2.18 (21.5)	2.11 (28.2)	2.12 (29.9)	2.12 (28.0)	2.12 (30.1)
$E_{\text{th}}(\text{SWCNT} \cdots \text{Au} \cdots \text{A} \cdots \text{T})$	14.05	29.83	23.1	21.5	42.3	44.0	57.8	60.0
Energy gap (eV)	0.85 (0.72) <sup>a</sup>	0.85	0.30	0.13	0.27	0.13	0.27	0.13
Mulliken charge (au.)								
$q(\text{A})$ and $q(\text{T})$	0.170	0.204 and –0.032 (0.046 and –0.046) <sup>b</sup>	–	–	0.276	0.271	0.291 and –0.010	0.295 and –0.017
$q(\text{Au})$	–0.170	–0.172	0.005	–0.005	0.123	0.122	0.128	0.122
$q(\text{SWCNT})$	–	–	–0.005	0.005	–0.399	–0.393	–0.408	–0.401
NPA charge (au.)								
$q(\text{A})$ and $q(\text{T})$	0.111	0.140 and –0.024 (0.039 and –0.039) <sup>c</sup>	–	–	0.153	0.152	0.167 and –0.014	0.172 and –0.018
$q(\text{Au})$	–0.111	–0.116	0.023	0.013	0.376	0.366	0.384	0.371
$q(\text{SWCNT})$	–	–	–0.023	–0.013	–0.529	–0.518	–0.538	–0.526
Dipole moment (debye)	3.281	3.904	2.676	2.662	8.074	8.658	9.342	10.441

<sup>a</sup> The energy gap of the Au atom.

<sup>b</sup> Mulliken charges of adenine and thymine molecules in the original A:T base pair.

<sup>c</sup> NPA charges of adenine and thymine molecules in the original A:T base pair.

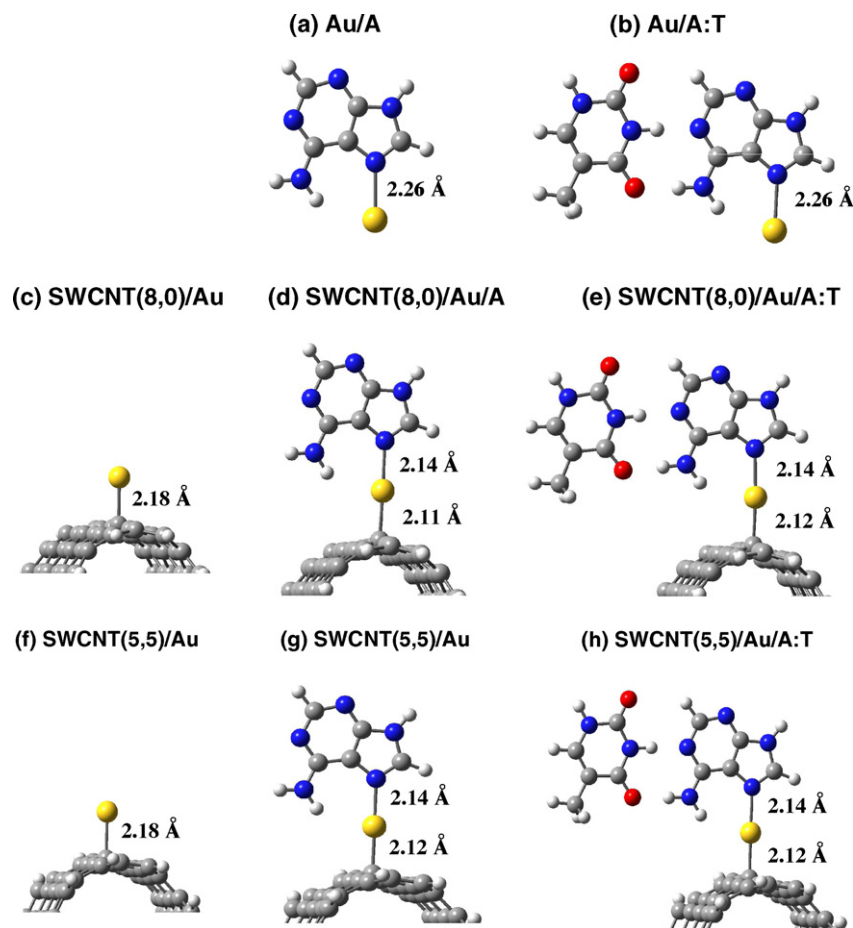


Fig. 5. Fully optimized geometries and Au–C and Au–N distances of the systems constructed from the most stable SWCNT/Au complexes (see Fig. 4).

Table 3

Geometrical parameters and atomic charges of an isolated adenine molecule and of the adenine in the complexes Au/A, SWCNT(8,0)/Au/A and SWCNT(5,5)/Au/A

	A	Au/A	SWCNT/Au/A	
			SWCNT (8,0) complex	SWCNT (5,5) complex
Distance (Å)				
$r(\text{N6-H6}')$	1.01	1.01	1.01	1.01
$r(\text{N6-H6}'')$	1.01	1.02	1.02	1.02
$r(\text{N6-Au})$	–	3.40	3.43	3.44
Angle (°)				
$\angle(\text{C6N6H6}')$	119.1	118.7	118.5	118.6
$\angle(\text{C6N6H6}'')$	120.1	120.1	120.9	120.8
Mulliken charge (au.)				
N7	–0.208	–0.307	–0.256	–0.253
C5	–0.032	0.071	0.060	0.054
C6	0.112	0.116	0.125	0.130
N1	–0.189	–0.180	–0.172	–0.181
N6	–0.184	–0.185	–0.178	–0.186
H6'	0.143	0.150	0.154	0.157
H6''	0.159	0.171	0.177	0.179
NPA charge (au.)				
N7	–0.443	–0.482	–0.502	–0.501
C5	–0.025	–0.014	–0.006	–0.006
C6	0.374	0.380	0.380	0.379
N1	–0.500	–0.488	–0.482	–0.483
N6	–0.729	–0.716	–0.711	–0.712
H6'	0.399	0.404	0.408	0.408
H6''	0.402	0.405	0.407	0.407



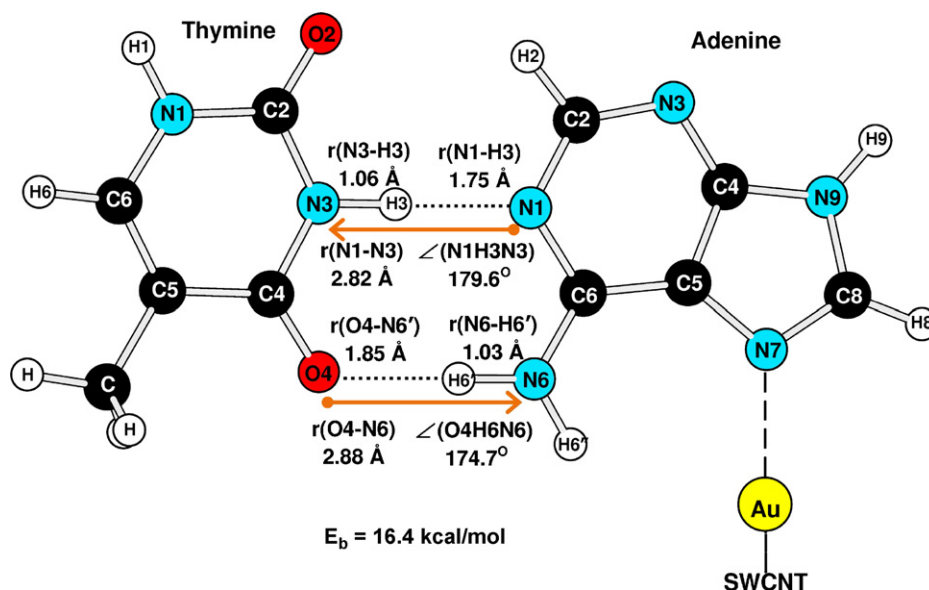


Fig. 6. Geometry of the double hydrogen bond of the original A:T base pair (as reference) and calculated binding energies ( $E_b$ ). The arrows show the directions of electron transfer.

structures. Even though the adenine base acquires a positive overall charge in the complexes, as noted above, its N7 atom is negatively charged compared to the one in isolated adenine. On interactions of the adenine base with Au and SWCNT/Au, the N1 atoms (which form a hydrogen bond with the H3 proton of the thymine base) become less negative charges, and the electrophilic protons at the H6' position become more positive. The  $\angle(\text{C6N6H6'})$  angle slightly decreases when the N6H6'...O4 hydrogen bond is formed with a thymine molecule. This should be an indication that Au and SWCNT/Au will cause a weaker hydrogen bonding at the N1 position and a stronger hydrogen bonding at the N6–H6' position of the base pairs.

### 3.3. SWCNT/gold/adenine:thymine complexes (target capture)

The final step in DNA sensor development is the evaluation of system stability (probe strand and analyte-target binding) and electronic sensitivity. Information concerning this topic is presented in Fig. 6 and Table 4.

#### 3.3.1. Stability

The binding of thymine with adenine only slightly perturbs both the adenine–Au and the Au–SWCNT interactions. Therefore, the Au/A:T and SWCNT/Au/A:T complexes maintain the stability of probe strands acting as the electronic delivery part. In all SWCNT/Au/A:T complexes, the A:T base pairs always arrange in a perpendicular direction to the SWCNTs alignments even if no symmetry constraints are applied (cf. Fig. 5). The analysis of the double hydrogen bonds in the isolated A:T base pair shows two significant electron transfer interactions. The first one is an electron transfer from a lone orbital of the N1 atom in adenine to an N3–H3 antibonding orbital in the thymine base (N3–H3 where the bond is

lengthened by 0.04 Å) and the second one is an electron transfer from the lone orbital of the O4 atom in thymine to a N6–H6' antibonding orbital in the adenine molecule (N6–H6' where the bond is lengthened by 0.02 Å). Compared to the isolated A:T base pair (Table 5),  $r(\text{N1-N3})$  is shorter than  $r(\text{O4-N6})$  and the  $\angle(\text{N1H3N3})$  bond angle is closer to the optimum interaction alignment of 180° than  $\angle(\text{O4H6N6})$ . This indicates that the strength of N1...H3–N3 interaction is greater than that of the O4...H6–N6 interaction.

Fig. 6 and Table 4 show the optimized geometrical parameters in the double hydrogen bonds region of the A:T base pair complexes. It is noted that the gold atom causes a weaker N3–H3...N1 hydrogen bond. This H-bond becomes even weaker when the gold atom is attached on a sidewall of the SWCNT. The distances between N3 and N1 in the N3–H3...N1 hydrogen bond are 2.82, 2.84, 2.86 and 2.85 Å for A:T, Au/A:T, SWCNT(8,0)/Au/A:T and SWCNT(5,5)/Au/A:T systems, respectively. The lengthened N1–N3 bonds correspond to the increasing of the N1–H3 bond distance and the decrease of the N3–H3 bond distance. Again, the O4...H6'–N6 H-bond behaves in the opposite way to the N3–H3...N1 H-bond. The O4–N6 distance is shortened from 2.88 Å to 2.87, 2.83 and 2.84 Å via interactions of the base pair with Au, SWCNT(8,0)/Au and SWCNT(5,5)/Au, respectively. Again, the shorter O4–N6 bond corresponds to the increased N6–H6' and the decreased O4–H6' bond distances. From the atomic partial charges it can be seen that, compared with the isolated A:T base pair, electron transfer from the adenine to thymine molecule is diminished in the complexes, as detailed in Table 4. Most of the binding energy changes correspond to the bond length modulations. The interactions of A:T base pairs are weakened from –16.4 kcal/mol to –15.8, –15.5 and –16.0 kcal/mol for Au/A:T, SWCNT(8,0)/Au/A:T and SWCNT(5,5)/Au/A:T complexes, respectively. The minute destabilization of the base pair (by 0.4–0.9 kcal/mol) can be explained by the competition

Table 4

Geometrical parameters, atomic charges and calculated binding energies ( $E_b$ ) of the double hydrogen bond of the original A:T base pair (as reference) and several target-probe systems

	A:T	Au/A:T	SWCNT/Au/A:T	
			SWCNT (8,0) complex	SWCNT (5,5) complex
Distance (Å)				
$r(\text{N1}-\text{N3})$	2.82	2.84	2.86	2.85
$r(\text{N1}-\text{H3})$	1.75	1.78	1.81	1.80
$r(\text{N3}-\text{H3})$	1.06 (1.02) <sup>a</sup>	1.06	1.05	1.06
$r(\text{O4}-\text{N6})$	2.88	2.87	2.83	2.84
$r(\text{O4}-\text{H6}')$	1.85	1.84	1.79	1.80
$r(\text{N6}-\text{H6}')$	1.03	1.03	1.04	1.04
Angle (°)				
$\angle(\text{N1H3N3})$	179.6	179.3	178.1	178.6
$\angle(\text{O4H6}'\text{N6})$	174.7	176.1	177.7	177.0
Mulliken charge (au.)				
N1	−0.207	−0.200	−0.205	−0.199
N6	−0.199	−0.209	−0.208	−0.210
H6'	0.180	0.184	0.188	0.190
H6''	0.150	0.167	0.181	0.178
O4	−0.354 (−0.290) <sup>a</sup>	−0.352	−0.346	−0.347
N3	−0.076 (−0.050) <sup>a</sup>	−0.078	−0.076	−0.066
H3	0.153 (0.141) <sup>a</sup>	0.149	0.157	0.148
NPA charge (au.)				
N1	−0.553	−0.539	−0.539	−0.539
N6	−0.721	−0.714	−0.701	−0.703
H6'	0.429	0.434	0.434	0.434
H6''	0.398	0.402	0.401	0.402
O4	−0.618 (−0.558) <sup>b</sup>	−0.609	−0.615	−0.615
N3	−0.590 (−0.589) <sup>b</sup>	−0.574	−0.588	−0.589
H3	0.445 (0.483) <sup>b</sup>	0.444	0.446	0.446
$E_b$ (A:T) (kcal/mol)	16.4	15.8	15.5	16.0

<sup>a</sup> Geometrical parameters and Mulliken charges of thymine base.

<sup>b</sup> Geometrical parameters and NPA charges of thymine base.

between a weakening of the N3–H3···N1 bond (bond shrinking and angle adjusting away from 180°) and a strengthening of the O4–H6'···N6 bond (bond stretching and angle adjusting close to 180°) in the A:T base pair.

### 3.3.2. Sensitivity

After the SWCNT/Au/A or Au/A probes are hybridized with the thymine molecule, we could not observe explicit changes of the HOMO-LUMO energy gaps. However, the sensitivity can

be explained in terms of charge transfer between target and the sensing probe. We could define some descriptors according to:

$$\Delta q_{\text{probe}}(\text{Au/A}) = q(\text{Au/A}) \text{ in } [\text{Au/A} : \text{T}] - q(\text{Au/A}) \text{ in } [\text{Au/A}] \quad (5)$$

$$\Delta q_{\text{probe}}(\text{SWCNT/Au/A}) = q(\text{SWCNT/Au/A}) \text{ in } [\text{SWCNT/Au/A} : \text{T}] - q(\text{SWCNT/Au/A}) \text{ in } [\text{SWCNT/Au/A}] \quad (6)$$

A larger value of  $\Delta q_{\text{probe}}$  should correspond to a higher sensitivity. However, both  $\Delta q_{\text{probe}}$  values result from gain and loss of charge from the thymine molecule. A positive value of the  $\Delta q_{\text{Mprobe}}$  parameter infers that the main contribution effect is the electrons transfer to the thymine molecule. Nevertheless, during a sensing process, electrons move from the thymine molecule to the adenine probe and these electrons are continuously transferred to the support and processed to be the output signal. Therefore, the parameter  $\Delta q_{\text{probe}}$  is not well suited for observing the electronic response. Accordingly, a quantity based on the alteration of the SWCNT/Au charges in

Table 5

The  $\Delta q_{\text{probe}}$ ,  $\Delta q_{\text{support}}$  and  $\Delta D$  parameters of Au/A:T, SWCNT(8,0)/Au/A:T and SWCNT(5,5)/Au/A:T

	Au/A:T		SWCNT/Au/A:T	
			SWCNT (8,0) complex	SWCNT (5,5) complex
$\Delta q$ Mulliken charge (au.)				
$\Delta q_{\text{probe}}$	0.032	0.010	0.017	
$\Delta q_{\text{support}}$	−0.002	−0.004	−0.008	
$\Delta q$ NPA charge (au.)				
$\Delta q_{\text{probe}}$	0.024	0.014	0.018	
$\Delta q_{\text{support}}$	−0.005	−0.001	−0.003	
$\Delta D$ (debye)	0.622	1.268	1.783	



SWCNT/Au/A and SWCNT/Au/A was defined as:

$$\Delta q_{\text{support}}(\text{Au}) = q(\text{Au}) \text{ in } [\text{Au}/\text{A} : \text{T}] - q(\text{Au}) \text{ in } [\text{Au}/\text{A}] \quad (7)$$

$$\begin{aligned} \Delta q_{\text{support}}(\text{SWCNT}/\text{Au}) \\ = q(\text{SWCNT}/\text{Au}) \text{ in } [\text{SWCNT}/\text{Au}/\text{A} : \text{T}] \\ - q(\text{SWCNT}/\text{Au}) \text{ in } [\text{SWCNT}/\text{Au}/\text{A}] \end{aligned} \quad (8)$$

The values of  $\Delta q_{\text{probe}}$  and  $\Delta q_{\text{support}}$  are listed in Table 5.  $\Delta q_{\text{support}}$  of the overall systems is very small,  $-0.001\text{e}$  and  $-0.008\text{e}$ , for Mulliken and NPA population analysis, respectively. Accordingly, the changes in the atomic partial charges upon binding of thymine are rather small and it might seem that the SWCNT has no effect on the hybridization. However, the change in the dipole moment (Eqs. (9) and (10)) that occurs when thymine binds to Au/A and to SWCNT/Au/A is quite significant. Table 5 also includes the two relevant changes in the dipole moment upon hybridization, without and with SWCNT, respectively.

$$\Delta D(\text{Au}) = D(\text{Au}/\text{A} : \text{T}) - D(\text{Au}/\text{A}) \quad (9)$$

$$\begin{aligned} \Delta D(\text{SWCNT}/\text{Au}) \\ = D(\text{SWCNT}/\text{Au}/\text{A} : \text{T}) - D(\text{SWCNT}/\text{Au}/\text{A}) \end{aligned} \quad (10)$$

It can be seen that, the change in the latter case is larger by a factor of about 2. This is due to the large electron affinity of the SWCNT (which itself has a dipole moment close to zero) and thus is not unexpected.

The fact that  $\Delta D$  is not reflected equally in the partial charges is not contradictory since the long distances of charge separation are reflected only in the dipole moment and both Mulliken and NPA charges are not bound to reproduce the dipole moment of the wave function. Both the amplification of the dipole moment and the distribution of charge from the Au/A:T subsystem into the SWCNT might be exploited by a suitable sensing mechanism.

#### 4. Conclusions

We performed DFT calculation on complexes of SWCNT/Au/A:T with both SWCNT(8,0) and SWCNT(5,5) and their subsystems. The SWCNT/Au hybrid structure has a higher sensor performance than a bare gold probe due to the electron gaining characteristics of the alternative integrated materials. The electron withdrawing property of the Au atom and SWCNT/Au causes a contraction of the N3–H3' ··· N1 hydrogen bond and a stretching of the O4–H6' ··· N6 one. However, the hydrogen bond alteration is insufficient to cause A:T base pair destabilization. The following effects were noted: (1) substantial stability of DNA probe immobilization; (2) measurable electrical signature of the target detection (distinct charge transfer or sensitive conductivity); (3) robustness of DNA hybridization. Both of the SWCNT(8,0)/Au and SWCNT(5,5)/Au materials have a similar performance with respect to these features. The other interesting function of the SWCNT/Au hybrid structure, beyond acting as the platform for

the adenine probe construction, is that it is the sensing material for nucleic acids. The SWCNT/Au structure could also act as sensing material for nucleic acids since it binds more strongly to adenine capturing than an isolated Au atom. Especially, the SWCNT(8,0)/Au/A complex can accelerate the transfer of electrons to the sensing part.

#### Acknowledgments

This research was supported by grants from the Thailand Research Fund, National Nanotechnology Center under the National Science and Technology Development Agency, Kasetsart University Research and Development Institute (KURDI), the National Nanotechnology Center (NANOTEC Center of Excellence and CNC Consortium) and the Commission on Higher Education, Ministry of Education under Postgraduate Education and Research Programs in Petroleum and Petrochemicals, and Advanced Materials.

#### References

- [1] T.G. Drummond, M.G. Hill, J.K. Barton, Electrochemical DNA sensors, *Nat. Biotechnol.* 21 (10) (2003) 1192–1199.
- [2] W. Vercouter, M. Akeson, Biosensors for DNA sequence detection, *Curr. Opin. Chem. Biol.* 6 (6) (2002) 816–822.
- [3] J. Wang, Electrochemical nucleic acid biosensors, *Anal. Chim. Acta* 469 (1) (2002) 63–71.
- [4] J. Zhai, C. Hong, R. Yang, DNA based biosensors, *Biotechnol. Adv.* 15 (1) (1997) 43–58.
- [5] M.-C. Daniel, D. Astruc, Gold nanoparticles: assembly, supramolecular chemistry, quantum-size-related properties, and applications toward biology, catalysis, and nanotechnology, *Chem. Rev.* 104 (1) (2004) 293–346 (Washington, DC, United States).
- [6] N.C. Tansil, Z. Gao, Nanoparticles in biomolecular detection, *Nanotoday* 1 (1) (2006) 28–37.
- [7] C.S. Thaxton, D.G. Georganopoulou, C.A. Mirkin, Gold nanoparticle probes for the detection of nucleic acid targets, *Clin. Chim. Acta* 363 (1–2) (2006) 120–126.
- [8] Z.-L. Zhang, D.-W. Pang, H. Yuan, R.-X. Cai, H.D. Abruna, Electrochemical DNA sensing based on gold nanoparticle amplification, *Anal. Bioanal. Chem.* 381 (4) (2005) 833–838.
- [9] H. Kimura-Suda, D.Y. Petrovykh, M.J. Tarlov, L.J. Whitman, Base-dependent competitive adsorption of single-stranded DNA on gold, *J. Am. Chem. Soc.* 125 (30) (2003) 9014–9015.
- [10] E.S. Kryachko, F. Remacle, Complexes of DNA bases and Watson–Crick base pairs with small neutral gold clusters, *J. Phys. Chem. B* 109 (48) (2005) 22746–22757.
- [11] H. Cai, X. Cao, Y. Jiang, P. He, Y. Fang, Carbon nanotube-enhanced electrochemical DNA biosensor for DNA hybridization detection, *Anal. Bioanal. Chem.* 375 (2) (2003) 287–293.
- [12] G. Gruner, Carbon nanotube transistors for biosensing applications, *Anal. Bioanal. Chem.* 384 (2) (2006) 322–335.
- [13] A. Merkoci, *Micro. Chim. Acta* 152 (3–4) (2006) 157–174.
- [14] A. Merkoci, M. Pumera, X. Llopis, B. Perez, M. del Valle, S. Alegret, New materials for electrochemical sensing VI: carbon nanotubes, *TrAC Trends Anal. Chem.* 24 (9) (2005) 826–838.
- [15] M. Valcarcel, B.M. Simonet, S. Cardenas, B. Suarez, Present and future applications of carbon nanotubes to analytical science, *Anal. Bioanal. Chem.* 382 (8) (2005) 1783–1790.
- [16] L. Jiang, L. Gao, Modified carbon nanotubes: an effective way to selective attachment of gold nanoparticles, *Carbon* 41 (15) (2003) 2923–2929.
- [17] L. Liu, T. Wang, J. Li, Z.-X. Guo, L. Dai, D. Zhang, D. Zhu, Self-assembly of gold nanoparticles to carbon nanotubes using a

- thiol-terminated pyrene as interlinker, *Chem. Phys. Lett.* 367 (5–6) (2002) 747–752.
- [18] X. Ma, X. Li, N. Lun, S. Wen, Synthesis of gold nano-catalysts supported on carbon nanotubes by using electroless plating technique, *Mater. Chem. Phys.* 97 (2–3) (2006) 351–356.
- [19] Y. Zhang, N.W. Franklin, R.J. Chen, H. Dai, Metal coating on suspended carbon nanotubes and its implication to metal-tube interaction, *Chem. Phys. Lett.* 331 (2000) 35–41.
- [20] S.H. Lim, J. Wei, J. Lin, Electrochemical genosensing properties of gold nanoparticle-carbon nanotube hybrid, *Chem. Phys. Lett.* 400 (4–6) (2004) 578–582.
- [21] J.P. Perdew, K. Burke, M. Ernzerhof, Generalized gradient approximation made simple, *Phys. Rev. Lett.* 77 (18) (1996) 3865–3868.
- [22] D. Andrae, U. Haeussermann, M. Dolg, H. Stoll, H. Preuss, Energy-adjusted ab initio pseudopotentials for the second and third row transition elements, *Theor. Chem. Acc.* 77 (2) (1990) 123–141.
- [23] M.J. Frisch, G.W. Trucks, H.B. Schlegel, G.E. Scuseria, M.A. Robb, J.R. Cheeseman, J.A. Jr. Montgomery, T. Vreven, K.N. Kudin, J.C. Burant, J.M. Millam, S.S. Iyengar, J. Tomasi, V. Barone, M. Mennucci, B. Cossi, G. Scalmani, N. Rega, G.A. Petersson, H. Nakatsuji, M. Hada, M. Ehara, K. Toyota, R. Fukuda, J. Hasegawa, M. Ishida, T. Nakajima, Y. Honda, O. Kitao, H. Nakai, M. Klene, X. Li, J.E. Knox, H.P. Hratchian, J.B. Cross, C. Adamo, J. Jaramillo, R. Gomperts, R.E. Stratmann, O. Yazyev, A.J. Austin, R. Cammi, C. Pomelli, J.W. Ochterski, P.Y. Ayala, K. Morokuma, G.A. Voth, P. Salvador, J.J. Dannenberg, V.G. Zakrzewski, S. Dapprich, A.D. Daniels, M.C. Strain, O. Farkas, D.K. Malick, A.D. Rabuck, K. Raghavachari, J.B. Foresman, J.V. Ortiz, Q. Cui, A.G. Baboul, S. Clifford, J. Cioslowski, B.B. Stefanov, G. Liu, A. Liashenko, P. Piskorz, I.L. Komaromi, R. Martin, D.J. Fox, T. Keith, M.A. Al-Laham, C.Y. Peng, A. Nanayakkara, M. Challacombe, P.M.W. Gill, B. Johnson, W. Chen, M.W. Wong, C. Gonzalez, J.A. Pople, Gaussian 03, Revision B.05, Gaussian, Inc., Wallingford CT, 2004.
- [24] R. Ahlrichs, M. Baer, M. Haeser, H. Horn, C. Koelmel, Electronic structure calculations on workstation computers: the program system TURBOMOLE, *Chem. Phys. Lett.* 162 (3) (1989) 165–169.
- [25] K. Eichkorn, O. Treutler, H. Oehm, M. Haeser, R. Ahlrichs, Auxiliary basis sets to approximate Coulomb potentials, *Chem. Phys. Lett.* 240 (4) (1995) 283–290;
- K. Eichkorn, O. Treutler, H. Oehm, M. Haeser, R. Ahlrichs, Auxiliary basis sets to approximate Coulomb potentials [Erratum], *Chem. Phys. Lett.* 242 (6) (1995) 652–660.
- [26] N.C. Seeman, J.M. Rosenberg, F.L. Suddath, J.J. Kim, A. Rich, RNA double-helical fragments at atomic resolution: I. The crystal and molecular structure of sodium adenylyl-3',5'-uridine hexahydrate, *J. Mol. Biol.* 104 (1) (1976) 109–144.
- [27] I.K. Yanson, A.B. Teplitskii, L.F. Sukhodub, Experimental studies of molecular interactions between nitrogen bases of nucleic acids, *Biopolymers* 18 (5) (1979) 1149–1170.
- [28] E. Durgun, S. Dag, V.M.K. Bagci, O. Gulseren, T. Yildirim, S. Ciraci, Systematic study of adsorption of single atoms on a carbon nanotube, *Phys. Rev. B: Condensed Matter Mater. Phys.* 67 (20) (2003), 201401/201401–201401/201404.
- [29] E.D. Glendening, J.K. Badenhoop, A.E. Reed, J.E. Carpenter, J.A. Bohmann, C.M. Morales, F. Weinhold, NBO 5.0, Theoretical Chemistry Institute, University of Wisconsin, Madison, WI, 2001, <http://www.chem.wisc.edu/~nbo5>.
- [30] P.J. Hay, W.R. Wadt, Ab initio effective core potentials for molecular calculations. Potentials for the transition metal atoms scandium to mercury, *J. Chem. Phys.* 82 (1) (1985) 270–283.